

Flow Structures of a Pseudoplastic Fluid in a Stirred Tank Using Particle Image Velocimetry

Jennifer Ayala¹, Aline Gallo De Mitri¹, Helder L. de Moura², Rodrigo de L. Amaral³, Grazielle Espina¹,
Guilherme J. de Castilho¹

¹Process Engineering Department, School of Chemical Engineering, University of Campinas
Albert Einstein Ave., 500 – Zip Code: 13083-852, Campinas-SP, Brazil
j192526@dac.unicamp.br; a093335@dac.unicamp.br; g198215@dac.unicamp.br; guijcas@unicamp.br

²Center for Petroleum Studies, University of Campinas
Cora Coralina st., 350 – Zip Code: 13083-896, Campinas-SP, Brazil
helderlima@feq.unicamp.br

³Department of Mechanical Engineering, POLI, University of São Paulo
Prof. Luciano Gualberto Ave., 380 – Zip Code: 05508-030, São Paulo-SP, Brazil
rodrigoamaral@usp.br

Abstract – Mixing is an important unit operation extensively applied in industrial processes involving fluid dynamics, thermal and chemical phenomena. The particle image velocimetry (PIV) approach has been widely used to study the flow patterns in stirred tanks. The majority of previous research relating to PIV in stirred tank has been restricted to determine the flow field based on measurements taken in a single vertical plane using Newtonian fluids. However, some flows of industrial interests are non-Newtonian. This work proposes to evaluate the flow structures of a pseudoplastic fluid, which is an aqueous solution of carboxymethylcellulose (CMC 0.55% p/p) by using angle-resolved (AR) PIV measurements in a stirred tank equipped with a four-blade 45° pitched-turbine (PBT) impeller. Two different impeller rotational speeds corresponding to low transitional (60 rpm, $Re \approx 80$) and high transitional regimes (840 rpm, $Re \approx 2900$) were employed. Four planes for fixed blade positions (angle-resolved measurements) of 0°, 22.5°, 45°, and 67.5°, set at 45° around the tank circumference were analyzed. Results are shown in terms of time-averaged velocity field and their axial and radial velocity components. For the low transitional regime, the radial component prevailed and the highest velocity values were found in the impeller discharge. For the high transitional regime, the flow was influenced by both radial and axial velocity components with fluid motion all over the tank. The angle-resolved measurements made it possible to verify that the low transitional regime flow is isotropic while the high transitional regime flow is anisotropic.

Keywords: Stirred tank, Pseudoplastic fluid, Transitional regime, Pitched blade turbine (PBT), PIV.

1. Introduction

Tanks with mechanical stirring are used in several industrial processes for solids suspension, gas dispersion, mixing and liquid emulsion. The growing interest in obtaining high-quality products at a low cost requires continuous improvements in the efficiency of the stirring system directly related to the understanding of the fluid dynamics behavior in agitated tanks. The majority of studies on stirred tanks tend to be limited to Newtonian fluids [1]–[4]. For these fluids, there are some guidelines for tank design in the literature. However, many mixing operations in industrial processes have high viscosity and non-Newtonian behavior. The main challenge for the operation with non-Newtonian fluids is related to their rheological characteristics. The shear stress and the shear rate present a non-linear relationship that can affect power consumption, mixing features, and mass transfer phenomena [5]. In order to study the flow patterns in mixing tanks, experimental techniques such as particle image velocimetry (PIV) have been widely used. PIV provides information about instantaneous velocity field in a selected plane by imaging the scattering of laser light from the tracer particles that accurately follow the motion of the fluid [6]. The determination of the velocity field can be performed through different PIV approaches in which it stands out ensemble-averaged and angle-resolved measurements. The main difference between those approaches is that ensemble-averaged considers the impeller blade position randomly or 360° rotation [7], [8] while

angle-resolved contemplates the periodicity of the flow due to the passage of the impeller blades by synchronizing the laser sheet with the blade position during the measurements [2], [8], [9]. The application of angle-resolved measurements allows a detailed investigation inside the stirred domain by analyzing different impeller blade positions.

The effect of the impeller blade position using angle-resolved PIV measurements in the flow of an aqueous solution of carboxymethyl cellulose (CMC 0.5 wt%) as a pseudoplastic fluid was studied. Experimental measurements in transitional regime were conducted using two rotational speeds (60 rpm and 840 rpm) in a tank stirred by a four-blade 45° PBT impeller and equipped with two equally spaced baffles. The flow structures in the time-averaged velocity field and their axial (\bar{v}) and radial (\bar{u}) components were analyzed.

2. Experimental

2.1. Experimental setup

Fig. 1. shows the agitated vessel and the experimental setup used for the PIV measurements. The pilot unit consists of an acrylic cylindrical tank with an inner diameter $T = 380$ mm with a 10% torispherical bottom head made of stainless steel 316-L. The 50 liters stirred tank was equipped with a four-blade 45° down-pumping PBT impeller ($D = 2T/5$, $C = T/3$) and four equally spaced baffles ($B = T/12$), as shown in Fig. 1 (b).

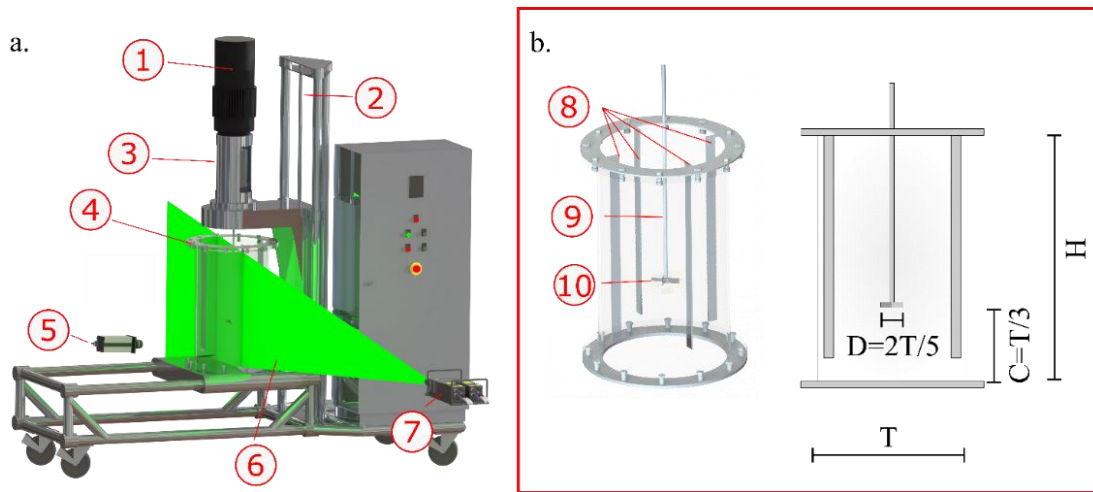


Fig. 1. (a) Experimental setup, (b) stirred tank. Legend: 1. Engine, 2. Shaft for impeller height adjustment, 3. Torque meter, 4. Tank, 5. Camera, 6. Light-sheet, 7. Laser, 8. Baffles, 9. Shaft, 10. Impeller PBT 45°. Ayala et al. [8].

The working fluid was an aqueous solution of carboxymethyl cellulose (CMC) sodium salt (0.5 wt% Sigma Aldrich High Viscosity with a degree of substitution 0.65-0.90). The stirred tank was filled to a height of 380 mm, that is, $H = T$ (square batch). The preparation and rheological characterization of the CMC solution was based on the study developed by Ayala et al. [8]. The fluid exhibited a shear-thinning behavior and can be described by the power-law model. Two rotational speeds (N) of the impeller were analyzed: 60 rpm and 840 rpm. An apparent average shear rate ($\dot{\gamma}$) has been calculated based on the Metzner Otto relationship [10], where the Metzner-Otto constant, k_s , for a down-pumping PBT has a value of 8.53 [11]. The flow conditions used for the experiments were determined based on the Reynolds number according to Eq. (1).

$$Re = \frac{\rho N^{2-n} D^2}{k(k_s)^{n-1}} \quad (1)$$

Table 1 presents the physical properties and the rheological parameters of the CMC as well as the impeller rotational speed and Reynolds number used in the experiments.

Table 1. Rheological properties of CMC fluid and flow conditions used in the experiments.

Experiment	Solution	Density ρ (kg·m ⁻³)	Refractive Index	Flow index n	Consistency Index k (Pa·s ^{n})	Rotational speed N (rpm)	Reynolds Number
A	CMC (0.5 wt%)	1000.380	1.334	0.559	0.737	60	80
B						840	2900

2.2. PIV system, Data Acquisition and Processing

The PIV system used was a classic 2D PIV acquired from Dantec Dynamics. The system includes a laser system Nd: YAG laser, 200 mJ, 532 nm applied with a light sheet thickness of 2 mm, one double frame image recording camera (FlowSense EO 8M-21 model, CCD sensor) with 15 Hz maximum frequency and 3312×2488 pixels resolution, a synchronizer and a computer with the Dynamic Studio software (version 6.9) for data acquisition. The tracer particles were silver-coated hollow glass spheres with a mean diameter of 10 μ m. In order to guarantee statistical reliability of PIV measurements, 1000 pairs of images for each area in double-frame mode with an interframe time of 150 μ s were recorded [8]. Pre-processing filters such as Intensity Capping, Local Minimum Intensity Subtraction (7×7 pixels) and Gaussian filter (3×3 pixels) were used to optimize the intensity distribution and the shape of the particle image in the frame. The images were initially processed using a multigrid analysis with discrete window offset [12][13]. The size of the initial interrogation window was 48 pixels with 25% overlap. In the multigrid analysis, five steps were used in the interrogation window. The first four consisted in gradually reducing by 25% all windows, except the last one that was reduced by 50%. The final interrogation window was $IW_f=1$ vector/10 px. The images were processed using the standard cross-correlation (SCC) method. The post-processing of the images was performed at the end of each step using an adaptation of the original median test to detect spurious PIV data developed by Westerweel and Scarano [14] to minimize the outliers and to avoid instabilities and noise propagation [8].

3. Results and Discussion

The PIV time-averaged velocity fields, constituted by the overlapping of axial (\bar{v}/U_{tip}) and radial (\bar{u}/U_{tip}) velocity fields and defined as $\overline{(v^2 + u^2)^{1/2}}/U_{tip}$, are shown in Fig. 2 for the case of the low transitional regime (60 rpm, Re = 80), for the four impeller blade positions obtained by angle-resolved measurements (AR 0°, AR 22.5°, AR 45° and AR 67.5°). The velocity vectors were normalized by the impeller tip velocity, defined as $U_{tip} = \pi DN \cong 0.48 \text{ m} \cdot \text{s}^{-1}$. The axial and radial positions were normalized by the height (H) of the liquid and by the tank radius (R), respectively. Fig. 2(a) shows that the time-averaged velocity distributions were similar for the different angle-resolved measurements, exhibiting a uniform jet flow towards the tank wall as the impeller blade moved forward. The highest velocity values were verified around the impeller and across the radial extension, reaching higher levels of approximately $\cong 0.4 U_{tip}$. Also, a poorly stirring region was presented in the region limited by $0.1 < z/H < 0.25$ and $0 < r/R < 0.8$. Fig 2 (b-c). In this region, the flow is predominantly radial. This result was expected, since the inefficiency in ensuring an axial agitation is a characteristic of the PBT impeller. It was also observed that when the jet hits the tank wall, the fluid loses velocity and is held back when the impact occurs.

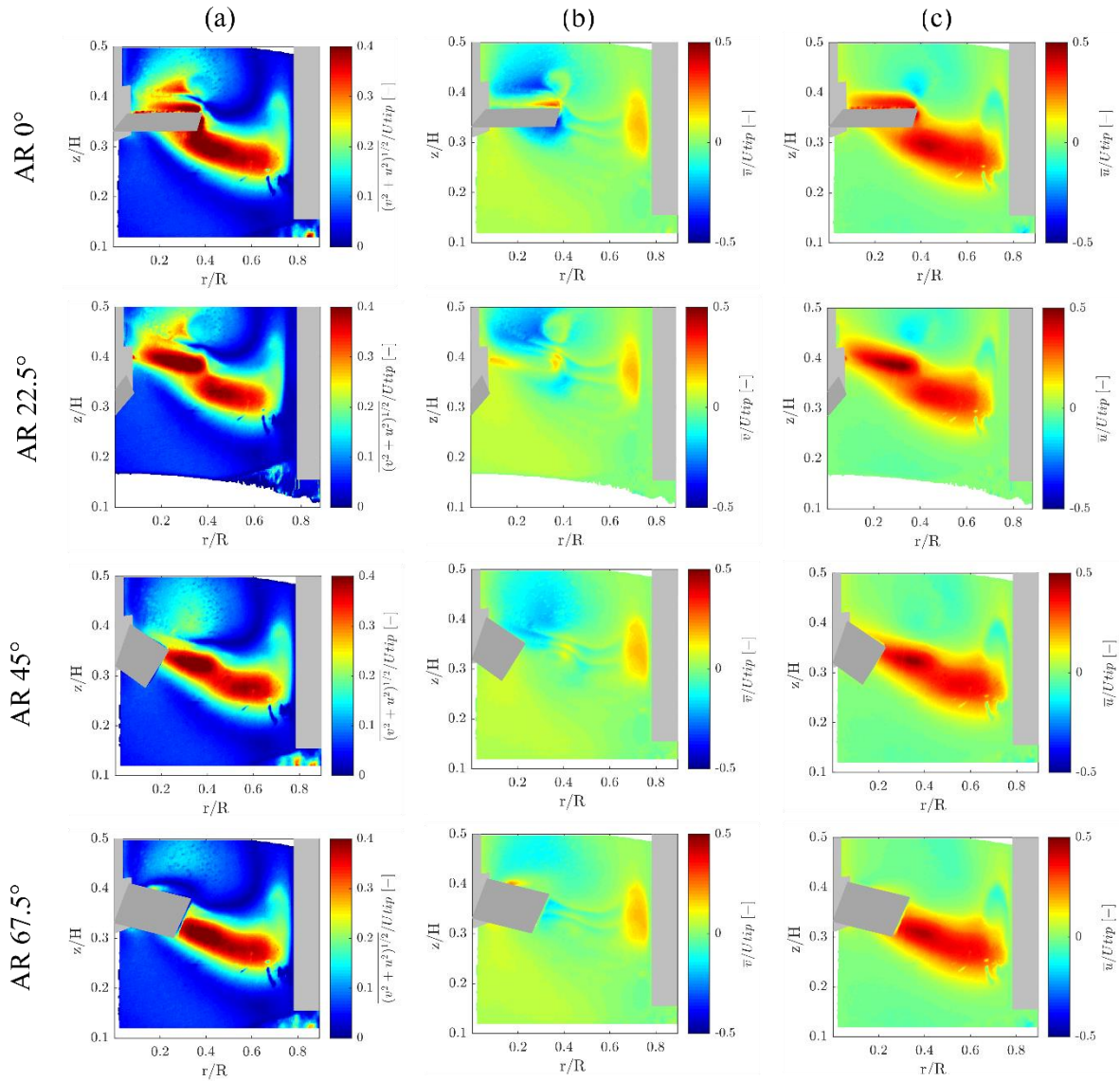


Fig. 2. Normalized time-averaged (a) velocity field $\left(\overline{(v^2 + u^2)^{1/2}}/U_{tip}\right)$, (b) axial velocity component (\bar{v}/U_{tip}) and (c) radial velocity component (\bar{u}/U_{tip}) for different angle-resolved PIV measurements and rotation speed of 60 rpm.

Fig. 3 presents the time-averaged velocity fields and their components for the four impeller blade positions obtained by angle-resolved measurements with impeller rotational speed of 840 rpm. The velocity vectors are normalized by the impeller tip velocity, $U_{tip} = \pi DN \cong 6.69 \text{ m} \cdot \text{s}^{-1}$. It can be verified that the high transitional regime ($Re = 2900$) intensifies the momentum transfer by increasing the shear rate and then reducing the fluid viscosity around the impeller. The time-averaged velocity fields (Fig. 3a) exhibited significant differences in velocity magnitude distribution and characteristics of trailing vortices as the impeller blade position moved in advance. This result indicates that the flow cannot be considered as isotropic in the tank domain. The trailing vortices induced by the impeller move from the suction region at the AR 0° to the suction region at AR 67.5° .

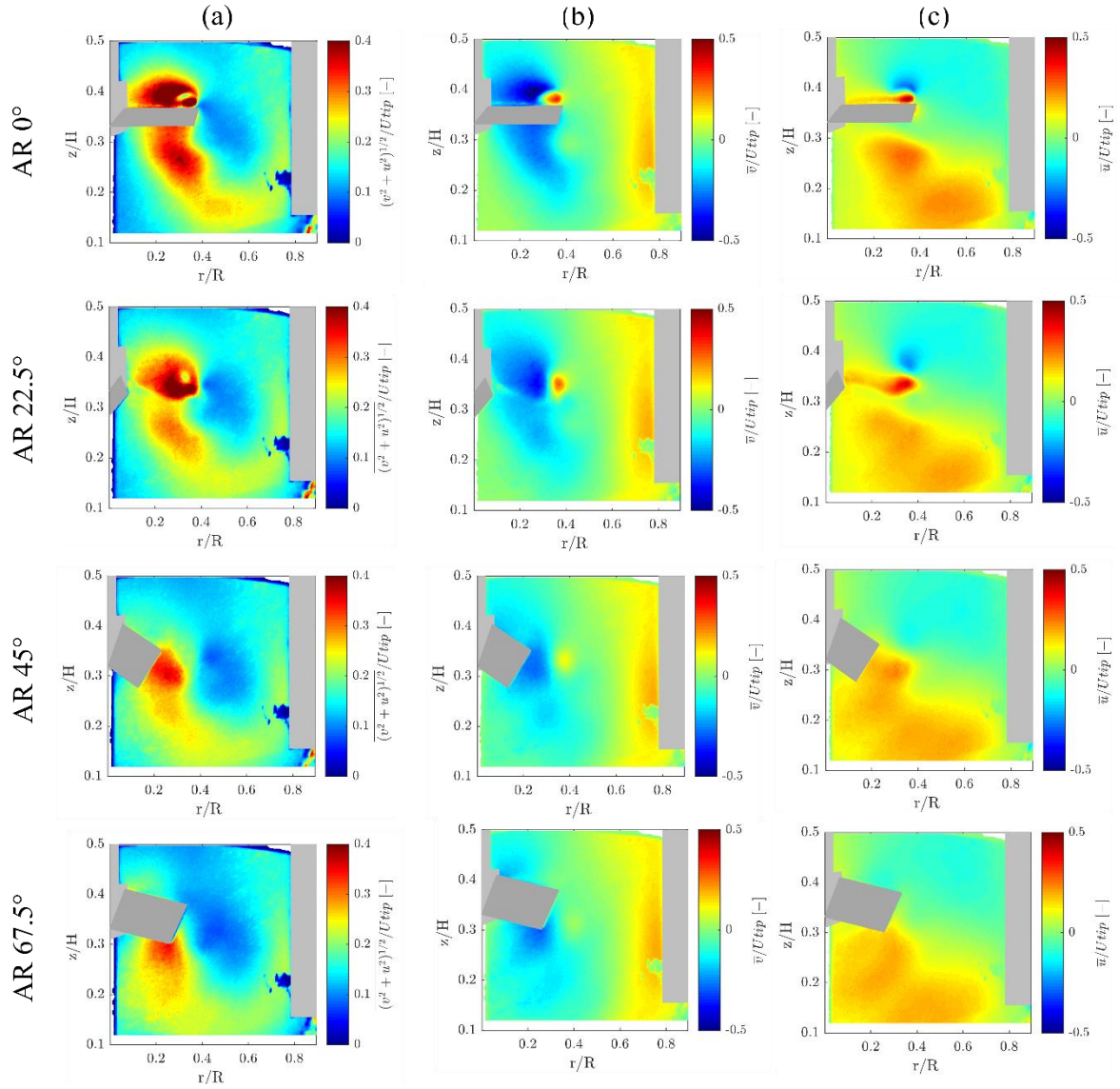


Fig. 3. Normalized time-averaged (a) velocity field $\left(\overline{(v^2 + u^2)^{1/2}}/U_{tip}\right)$, (b) axial velocity component (\bar{v}/U_{tip}) and (c) radial velocity component (\bar{u}/U_{tip}) for different angle-resolved PIV measurements and rotation speed of 840 rpm.

The time-averaged velocity magnitude presented a maximum in the region near the impeller tip. The maximum values were found as $\sim 0.4 U_{tip}$ at AR 0° . The time-averaged velocity in the circulation loop region had a minimum of $0.2U_{tip}$ for all AR measurements. According to Gabriele et al. [2], velocities near the impeller are sensitive to the angle relative to the blade and this region the flow moves slightly upwards and away from the impeller as the angle increases. Fig 3 (b-c) shows that both axial and radial velocity components influenced the flow. Despite the multigrid strategy application in the image processing, it was impossible to correct the noises generated by some physical imperfections at the bottom of the tank wall, as it can be clearly seen in the time-averaged velocity fields. However, those noises have not significantly impacted the representativeness of the fields neither the flow continuity.

Fig. 4 compares time-averaged velocity fields between both low transitional regime (60 rpm) and high transitional regime (840 rpm) for angle-resolved measurements at AR 0° and AR 45° . The time-averaged velocity distributions revealed a significant difference in velocity magnitude and in the jet shape formed around the impeller blade. For the rotation speed of 60 rpm, the flow was predominantly radial with high-velocity gradients in the impeller discharge region. In comparison, for the rotation speed of 840 rpm, the flow was influenced by both axial and radial velocity components,

and all the fluid was in movement inside de tank domain. Additionally, it was possible to verify the fluid resistance to deformation when compared AR 0° and AR 45° at 840 rpm. The vortex above de impeller blade fades as the impeller blade moves forward, and the velocity magnitude decrease in the circulation loop. This reveals anisotropic characteristics in the high transitional regime.

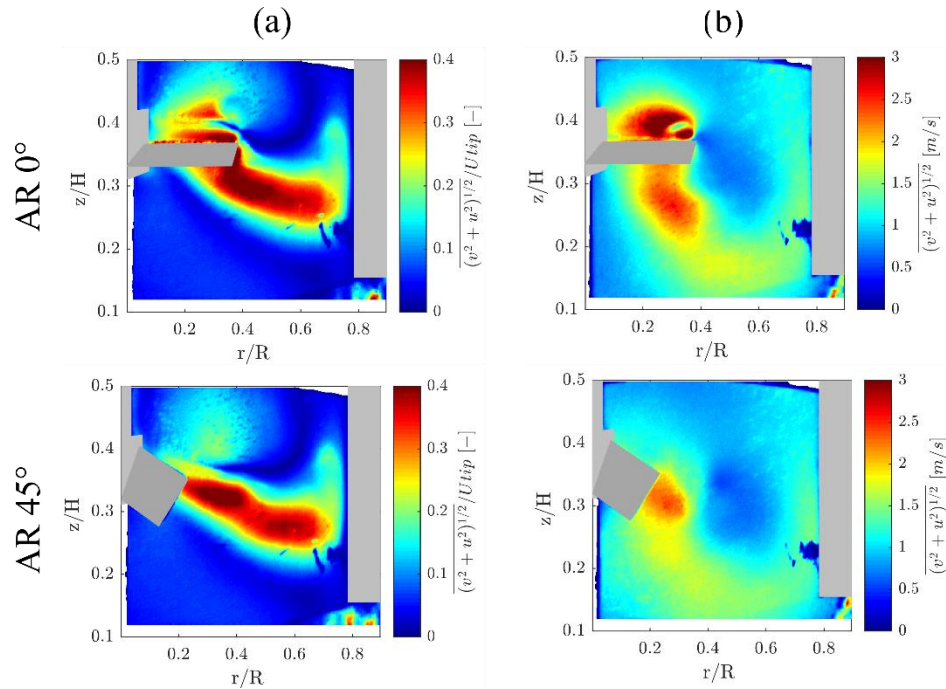


Fig. 4. Comparison of time-averaged velocity fields for both (a) transitional regime (60 rpm) and (b) high transitional regime (840 rpm) at AR 0° and AR 45°.

4. Conclusion

2D angle-resolved PIV experiments in a tank stirred by a pitched four-blade impeller were performed to analyze the effect of two rotational impeller speeds (60 rpm and 840 rpm) and four impeller blade positions (AR 0°, AR 22.5°, AR 45° and AR 67.5°) in the flow field of a pseudoplastic fluid (CMC solution). The time-averaged velocity fields in the low transitional regime ($Re = 80$) show that the flow is predominantly radial. For this condition, the inefficiency of the impeller in ensuring axial agitation was observed, which is a characteristic of the PBT impeller. On the other hand, the time-averaged velocity fields in the high transitional regime ($Re = 2900$) indicate that both axial and radial velocity components influenced the flow. The results for different impeller blade positions showed that the flow is isotropic in the low transitional regime. Nevertheless, the flow in high transitional regime exhibited significant differences in the velocity magnitude distribution and characteristics of trailing vortices when the impeller blade position moved forward, indicating anisotropy of the flow in the tank domain.

Acknowledgments

This study was sponsored by Petroleo Brasileiro S/A – PETROBRAS (process number 2017/00376-1) and was financed in part by the CAPES Higher Education Improvement Coordination - Finance Code 001, and the National Council for Scientific and Technological Development (CNPq; process number 140997/2019-9). The authors also would like to acknowledge the PIV_br (www.piv.eng.br) team for the support on the image processing.

References

- [1] S. Baldi and M. Yianneskis, “On the quantification of energy dissipation in the impeller stream of a stirred vessel

- from fluctuating velocity gradient measurements,” *Chem. Eng. Sci.*, vol. 59, no. 13, pp. 2659–2671, 2004, doi: 10.1016/j.ces.2004.03.021.
- [2] A. Gabriele, A. W. Nienow, and M. J. H. Simmons, “Use of angle resolved PIV to estimate local specific energy dissipation rates for up- and down-pumping pitched blade agitators in a stirred tank,” *Chem. Eng. Sci.*, vol. 64, no. 1, pp. 126–143, 2009, doi: 10.1016/j.ces.2008.09.018.
- [3] A. Guida, A. W. Nienow, and M. Barigou, “The effects of the azimuthal position of the measurement plane on the flow parameters determined by PIV within a stirred vessel,” *Chem. Eng. Sci.*, vol. 65, no. 8, pp. 2454–2463, 2010, doi: 10.1016/j.ces.2009.12.012.
- [4] A. Delafosse, M. L. Collignon, M. Crine, and D. Toye, “Estimation of the turbulent kinetic energy dissipation rate from 2D-PIV measurements in a vessel stirred by an axial Mixel TTP impeller,” *Chem. Eng. Sci.*, vol. 66, no. 8, pp. 1728–1737, 2011, doi: 10.1016/j.ces.2011.01.011.
- [5] R. P. Chhabra and J. F. Richardson, *Non-Newtonian Flow and Applied Rheology*. Oxford, 2008.
- [6] M. Raffel, C. E. Willert, F. Scarano, C. J. Kähler, Steven T. Wereley, and J. Kompenhans, *Particle Image Velocimetry*, Third Edit. Springer International Publishing, 2018.
- [7] X. Pan, L. Ding, P. Luo, H. Wu, Z. Zhou, and Z. Zhang, “LES and PIV investigation of turbulent characteristics in a vessel stirred by a novel long-short blades agitator,” *Chem. Eng. Sci.*, vol. 176, pp. 343–355, 2018, doi: 10.1016/j.ces.2017.10.054.
- [8] J. Ayala; H. L. de Moura; R. de L. Amaral; F. de A. O. Júnior; J. R. Nunhez, and G. J. de Castilho, “Two-dimensional shear rate field and flow structures of a pseudoplastic fluid in a stirred tank using particle image velocimetry,” *Chem. Eng. Sci.*, 2021.
- [9] R. Escudié and A. Liné, “Experimental analysis of hydrodynamics in a radially agitated tank,” *AIChE J.*, vol. 49, no. 3, pp. 585–603, 2003, doi: 10.1002/aic.690490306.
- [10] A. B. Metzner and R. E. Otto, “Agitation of non-Newtonian fluids,” *AIChE J.*, vol. 3, no. 1, pp. 3–10, 1957, doi: 10.1002/aic.690030103.
- [11] V. E. Márquez-Baños, A. D. De La Concha-Gómez, J. J. Valencia-López, A. López-Yáñez, and J. Ramírez-Muñoz, “Shear rate and direct numerical calculation of the Metzner-Otto constant for a pitched blade turbine,” *J. Food Eng.*, vol. 257, no. March, pp. 10–18, 2019, doi: 10.1016/j.jfoodeng.2019.03.021.
- [12] A. D. Barbutti, R. de L. Amaral, H. L. de Moura, F. de A. O. Júnior, J. R. Nunhez, and G. J. de Castilho, “A new field correction method for PIV measurements based on mutual information: Case study on a stirred tank flow,” *Meas. J. Int. Meas. Confed.*, vol. 186, no. March, 2021, doi: 10.1016/j.measurement.2021.110130.
- [13] F. Scarano, “Iterative image deformation methods in PIV,” *Meas. Sci. Technol.*, vol. 13, no. 1, pp. R1–R19, Jan. 2002, doi: 10.1088/0957-0233/13/1/201.
- [14] J. Westerweel and F. Scarano, “Universal outlier detection for PIV data,” *Exp. Fluids*, vol. 39, no. 6, pp. 1096–1100, Dec. 2005, doi: 10.1007/s00348-005-0016-6.